

Pressure-Level Dependency and Densification Behavior of Sand Through Generalized Plasticity Model

Hoe I. Ling, M.ASCE,¹ and Huabei Liu²

Abstract: Natural soil deposits and man-made earth structures exhibit complicated engineering behavior that is influenced by factors such as the stress level and drainage conditions. The stress conditions within a soil structure vary greatly, ranging from very low to very high values, due to the dead weight, loading and boundary conditions. Saturated sand deposits that exhibit drained conditions under static loading become undrained when subject to earthquake excitations. The Pastor–Zienkiewicz–Chan model has demonstrated considerable success in describing the inelastic behavior of soils under isotropic monotonic and cyclic loadings, including liquefaction and cyclic mobility. This study proposed modifications to the Pastor–Zienkiewicz–Chan model so that effects of stress level and densification behavior are simulated. The proposed model suggested that the angle of internal friction, elastic and plastic moduli are dependent on the pressure levels. Relevant modifications were made to incorporate a power term of mean effective stress on the loading plastic modulus so that a stress-level dependent volume change is obtained in combination with the stress-dilatancy relationship. To better simulate cyclic loading with reference to densification behavior, an exponential term of plastic volumetric strain is included for the unloading and reloading plastic moduli. A total of 11 parameters are needed for monotonic loading, whereas 15 parameters are needed in describing the cyclic behavior. The model simulations were compared with undrained and drained triaxial test results of several kinds of sand under dense and loose states. The predictive capability for monotonic and cyclic loading conditions was also demonstrated.

DOI: 10.1061/(ASCE)0733-9399(2003)129:8(851)

CE Database subject headings: Plasticity; Constitutive models; Densification; Cyclic loads; Sand.

Introduction

It is well known that sands respond differently to the variation in confining stress and densities. Experimental investigation has shown that when a sand is sheared under high confining pressure, a large reduction in the volume and angle of internal friction may result (Vesic and Clough 1968; Banks and MacIver, 1969; Miura et al. 1984; Bolton 1986; Lade and Yamamuro 1996; Yamamuro and Lade 1996) because of the crushing of soil particles. The behavior of sand under very low confining pressure has also been studied by several researchers (Ponce and Bell 1971; Fukushima and Tatsuoka 1984; Tatsuoka et al. 1986; Maeda and Miura 1999). The test results showed a dilatant deformation behavior and the angle of internal friction increased markedly as the confining pressure was reduced. The test results covering a wide range of pressures led to a similar conclusion (Lee and Seed 1967; Verdugo and Ishihara 1996).

Another significant property of sand is related to the densification and hardening behavior under repeated loadings (Silver

and Seed 1971; Luong 1980; Pradhan 1989). This behavior influences the permanent deformation and damping of soil structures under dynamic and cyclic loadings. Following an increase in the number of cycles of loading, in sand, the stiffness increases while the damping reduces, thus affecting the dynamic response of the soil structures. Attempts have also been made to incorporate this effect into sand models (Cuellar et al. 1977; Boyce 1980; Bouckovalas et al. 1986; Dobry and Petrakis 1990).

Traditionally, soil constitutive models have been developed separately for clay and sand. Classical plasticity, kinematic hardening plasticity, and bounding surface plasticity have been utilized to simulate sand behavior. In these theories, the yield surface and plastic potential are defined explicitly. In better simulating the soil behavior, complicated yield surfaces and plastic potentials as well as hardening rules were proposed (e.g., Prevost 1978; Vermeer 1978; Nova and Wood 1979; Lade and Kim 1988; Bardet 1986; Dafalias 1986; Tatsuoka et al. 1993; Wan and Guo 1998; Li et al. 1999). The critical state concept has been used in an attempt to unify the models for sands covering a wide range of densities through the state parameter (e.g., Been and Jefferies 1985; Wang et al. 1990; Jefferies 1993; Crouch et al. 1994; Manzari and Dafalias 1997). Recently, unified models for sand and clay have also been proposed (e.g., Crouch and Wolf 1994; Pestana and Whittle 1999), but they are relatively complicated, especially the Crouch–Wolf model which requires a large number of 25 parameters. Some of these advanced models were successful for monotonic loading conditions.

One of the models that is simple and yet demonstrating considerable success in modeling the cyclic behavior of sand under earthquake loading, including liquefaction and cyclic mobility, is the generalized plasticity model. This theory was introduced and applied to geomaterials by Mroz and Zienkiewicz (1984) and

¹Associate Professor, Dept. of Civil Engineering and Engineering Mechanics, Columbia Univ., 500 West 120th St., New York, NY 10027. E-mail: ling@civil.columbia.edu

²Graduate Research Assistant, Dept. of Civil Engineering and Engineering Mechanics, Columbia Univ., 500 West 120th St., New York, NY 10027.

Note. Associate Editor: Victor N. Kaliakin. Discussion open until January 1, 2004. Separate discussions must be submitted for individual papers. To extend the closing date by one month, a written request must be filed with the ASCE Managing Editor. The manuscript for this paper was submitted for review and possible publication on February 22, 2002; approved on December 4, 2002. This paper is part of the *Journal of Engineering Mechanics*, Vol. 129, No. 8, August 1, 2003. ©ASCE, ISSN 0733-9399/2003/8-851–860/\$18.00.

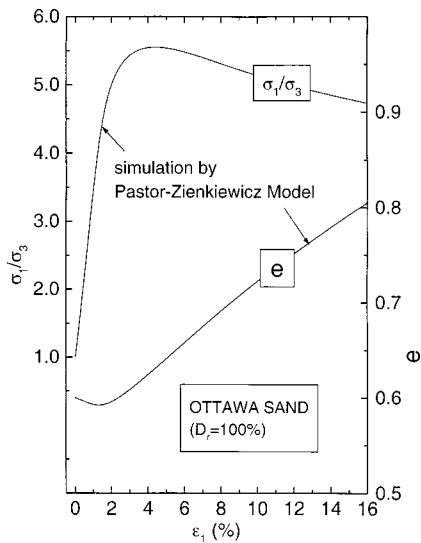


Fig. 1. Simulation of stress–strain relationships for drained triaxial tests using Pastor–Zienkiewicz–Chan model

Zienkiewicz and Mroz (1984), and was later extended by Zienkiewicz et al. (1985) and Pastor et al. (1985, 1986, 1990). In the generalized plasticity theory, the yield surface and plastic potential are not explicitly defined. Instead, direction vectors are used. With appropriate laws for the direction of plastic flow, loading–unloading directions and plastic moduli, salient behavior of soil can be described. Thus, generalized plasticity allows a less complicated simulation of experimental results for different loading conditions.

Pastor–Zienkiewicz–Chan model (Pastor et al. 1990), hereafter known as base model, exhibited several serious limitations in simulating pressure dependency and densification behavior of sand under cyclic loading. Fig. 1 shows the stress–strain response of a dense sand under drained triaxial compression. The parameters for the dense sand were calibrated by Pastor et al. (1990) for a confining stress of 207 kPa, but the model gives the same stress–strain response for all confining pressures. Fig. 2 shows the results of a loose sand using the parameters given by Pastor and Zienkiewicz (1986). The base model does not simulate the hardening behavior of sand under cyclic loading, since the stiffness and damping do not change with the cycles of loading.

Recently, several modifications to the generalized plasticity model have been proposed (Pastor et al. 1993; Sassa and Sekiguchi 2001). In Pastor et al. (1993), anisotropy was considered, whereas in Sassa and Sekiguchi (2001), the effects of principle stress rotation were included. But these different versions of sand model still lack the capability to simulate the stress-dependent and densification behavior. In Pastor et al. (1993), densification was considered but the hardening effect was not simulated satisfactorily. Bahda et al. (1997) developed a slightly different version of generalized plasticity model using a new state parameter with double hardening rules.

In this paper, based on the work of Pastor et al. (1990), the generalized plasticity model was extended to include pressure dependency and densification behavior of sand under monotonic and cyclic loadings. The predictive capability of the proposed model was examined by comparing the simulations of loose and dense sands with the triaxial test results under both drained and undrained conditions.

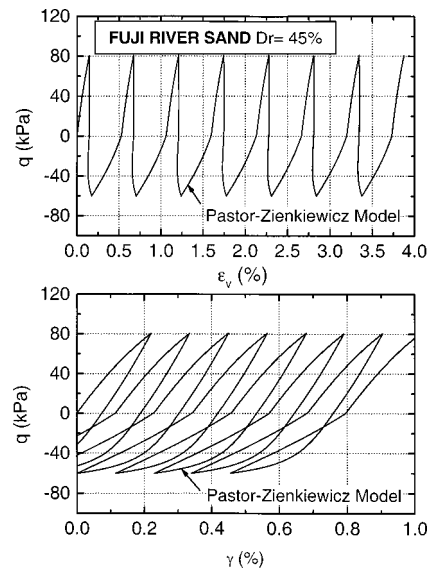


Fig. 2. Simulation of drained cyclic loading test using Pastor–Zienkiewicz–Chan model

Model Descriptions

In the generalized plasticity model, the total strain increment is divided into elastic and plastic components

$$d\epsilon = d\epsilon^e + d\epsilon^p \quad (1)$$

where $d\epsilon$, $d\epsilon^e$, and $d\epsilon^p$ = total, elastic, and plastic strain increments, respectively.

Nonlinear elasticity and theory of generalized plasticity are used to determine the relationships between incremental stresses and strains. The incremental stress–strain relationship is expressed as

$$d\sigma = \mathbf{D}^{ep} : d\epsilon \quad (2)$$

where $d\sigma$ and \mathbf{D}^{ep} = incremental stress tensor and elastoplastic stiffness tensor, respectively. Effective stresses are considered throughout this paper.

The elastoplastic stiffness tensor is given as (Mroz and Zienkiewicz 1984)

$$\mathbf{D}^{ep} = \mathbf{D}^e - \frac{\mathbf{D}^e : \mathbf{n}_{gL/U} : \mathbf{n}^T : \mathbf{D}^e}{H_{L/U} + \mathbf{n}^T : \mathbf{D}^e : \mathbf{n}_{gL/U}} \quad (3)$$

where \mathbf{D}^e , \mathbf{n} , $\mathbf{n}_{gL/U}$, and $H_{L/U}$ = elastic stiffness tensor, loading direction vector, flow direction vector under loading or unloading conditions, and loading or unloading plastic modulus, respectively.

Elastic Behavior

The elastic behavior is defined by the shear and bulk moduli (G_{\max} and K_{\max}), both dependent on the stress level. In the formulation of the base model, the elastic shear modulus is expressed as $G_{\max} = G_0(p'/p_a)$, where G_0 = shear modulus number and p' = mean effective stress, which is normalized by the atmospheric pressure p_a . The expression of Hardin and Richart (1963) is adopted where G_{\max} is related to normalized mean stress with an exponent equal to 0.5

$$G_{\max} = G_0(p'/p_a)^{0.5} \quad (4)$$

Note that G_0 is a function of initial void ratio (e.g., Ishihara 1996).

The Poisson's ratio is assumed constant for different mean stresses so that the bulk modulus is expressed as

$$K_{\max} = K_0(p'/p_a)^{0.5} \quad (5)$$

where K_0 = bulk modulus number.

The pressure dependency of moduli on power law may be unconservative and is a violation of the principle of thermodynamics (Zytynski et al. 1978; Boyce 1980), which requires that the bulk modulus also depends on the shear modulus. Since the experimental link between the bulk and shear moduli is weak and the soil may not be isotropic, Eqs. (4) and (5) are adopted solely based on an experimental standpoint. Note that the moduli have also been modified to satisfy the principle of thermodynamics (e.g., Boyce 1980; Houlsby 1985; Hueckel et al. 1992; Pestana and Whittle 1999).

The improvements related to the plastic behavior of generalized plasticity model are described as follows.

Stress Dilatancy

Several stress-dilatancy relationships have been proposed for sands (e.g., Rowe 1962; Nova and Wood, 1979; Bolton 1986). With reference to the rule of Nova and Wood (1979), Pastor et al. (1985) adopted the following generalized expression for monotonic loading of sand:

$$d_g = \frac{d\varepsilon_v^p}{d\varepsilon_s^p} = (1 + \alpha)(M_g - \eta) \quad (6)$$

where $d\varepsilon_v^p$ and $d\varepsilon_s^p$ = incremental plastic volumetric and deviatoric strains, respectively. M_g = slope of the critical state line on $p'-q$ plane, $\eta = q/p'$ = stress ratio, and α = model parameter.

M_g is related to the angle of internal friction at the critical state ϕ_{cv} and Lode's angle θ

$$M_g = \frac{6 \sin \phi_{cv}}{3 - \sin \phi_{cv} \sin 3\theta} \quad (7)$$

M_g is independent of confining stress but η varies with the pressure level (since q and p' do not change in the same ratio for nonproportional shearing), thus the dilatancy characteristics of sand under different mean effective stresses can be described through Eq. (6). Eq. (6) shows that dilatancy is zero at $\eta = M_g$, which represents the characteristic state line or line of phase transformation (Tatsuoka 1972; Ishihara 1996). The line of phase transformation determines if the volumetric deformation behavior will become contractive or dilative, and thus the generation of excess pore pressure. This is a simplification with the merit of keeping the number of parameters low, although experimentally the line of phase transformation, which may also depend on the total stress path, is slightly different from that of the critical state (e.g., Ibsen 1999).

Plastic Flow

The plastic flow direction under loading \mathbf{n}_{gL} is given in the triaxial space as

$$\mathbf{n}_{gL} = \left(\frac{d_g}{\sqrt{1+d_g^2}}, \frac{1}{\sqrt{1+d_g^2}} \right)^T \quad (8)$$

The nonassociate flow rule is followed so that the loading direction is expressed as

$$\mathbf{n} = \left(\frac{d_f}{\sqrt{1+d_f^2}}, \frac{1}{\sqrt{1+d_f^2}} \right)^T \quad (9)$$

where $d_f = (1 + \alpha)(M_f - \eta)$ and M_f is independent of the confining stress but dependent on the Lode angle [similar expression to M_g of Eq. (7)]. Thus, d_f varies with the mean effective stress for any strain levels.

Plastic Modulus for Loading, Unloading, and Reloading

The plastic modulus under monotonic loading H_L is modified by, first, including a power term containing normalized mean effective stress

$$H_L = H_0(p'/p_a)^{0.5} H_f \{H_v + H_s\} \quad (10)$$

where H_0 = plastic modulus number; and H_f , H_v , and H_s = plastic coefficients.

The plastic coefficients H_f and H_v are related to the failure and phase transformation lines. They show a decrease in value with an increase in the shear stress ratio

$$H_f = \left(1 - \frac{\eta}{\eta_f} \right)^4 \quad (11)$$

$$\eta_f = \left(1 + \frac{1}{\alpha} \right) M_f \quad (12)$$

$$H_v = 1 - \frac{\eta}{M_g} \quad (13)$$

where η_f = stress ratio parameter.

In the base model, the plastic coefficient H_s is expressed as $H_s = \beta_0 \beta_1 \exp(-\beta_0 \xi)$, where $\xi = \int |d\varepsilon_s^p|$ is the accumulative plastic deviatoric strain. In the proposed model, the following expression is used:

$$H_s = \beta_1 \exp \left(\frac{K_s \left(\frac{p'}{p_a} - 1 \right)}{\beta \cdot \xi} \right) \quad (14)$$

where the exponential term containing k_s is introduced to account for the pressure-dependent behavior of the strain level at peak strength. β_1 is a function of mean effective stress p' and stress ratio η

$$\beta_1 = \beta_{10} \frac{\eta_p / M_g - 1}{\eta_{p0} / M_g - 1} \quad (15)$$

where η_{p0} = peak value of stress ratio (η_p) at reference stress, which is taken at p_a . For isotropic compression test, the stress ratio $\eta = 0.0$, thus β_1 remains constant. For very loose sand, at peak strength $\eta = M_g$ and $\beta_1 = \beta_{10}$. For medium and dense sands, the peak strength is determined using the peak angle of internal friction ϕ through the well-known expression following Duncan et al. (1980), who used σ_3 instead of p'

$$\phi = \phi_0 - \Delta \phi \log_{10}(p'/p_a) \quad (16)$$

where ϕ_0 = peak angle of internal friction at atmospheric pressure and $\Delta \phi$ = change of angle for a 10-fold increase in the pressure.

Since β_1 depends on the confining pressure, the peak strength naturally depends on the stress level. Thus, by allowing the load-

Table 1. Material Parameters for Different Kinds of Sand

	Toyoura				Sacramento River ^c		Fontainebleau ^d	Fuji River ^e
	Very dense ^a	Dense ^b	Medium loose ^b	Very loose ^b	Dense	Loose	Dense	Loose
$e (D_r)$	0.67 (82.5%)	0.735 (63.7%)	0.833 (37.9 %)	0.907 (18.5%)	0.61 (100%)	0.87 (38%)	0.633 (65%)	0.737 (—)
$\phi_{p0} (^\circ)$	43.7	40.4	35.0	33.5	44.4	35.9	41.0	37.0
$\Delta\phi (^\circ)$	4.9	6.0	3.1	2.5	6.0	2.4	2.0	1.0
M_g	1.25	1.25	1.25	1.25	1.3	1.3	1.2	1.2
M_f	0.688	0.87	0.54	0.466	0.736	0.55	0.8	0.55
G_0/p_a	9,400	3,600	2,900	2,100	10,600	4,100	28,900	1,800
K_0/p_a	9,700	4,200	2,900	2,500	12,400	5,000	21,700	1,100
k_s	0.015	0.0	0.0	0.0	0.016	0.042	0.03	0.01
β_{10}	1.0	2.1	3.2	15.0	0.6	0.5	0.7	3.1
β_0	15	10.0	20.0	40.0	8	7	5	11.0
α	0.5	0.45	0.45	0.45	0.45	0.45	0.45	0.45
H_0/p_a	50,000	15,000	18,000	4,000	100,000	30,000	10,000	2,620
H_{u0}/p_a	40,000		20,000				7,000	2,830
r	3.0		5.0				1.0	0.1
r_u	1.0		0.0				0.0	5
r_d	3,000.0		10.0				180.0	22.0

^aFukushima and Tatsuoka (1984).

^bVerdugo and Ishihara (1996).

^cLee and Seed (1967).

^dLuong (1980).

^eTatsuoka (1972).

ing plastic modulus to depend on p' and by introducing k_s , together with the dilatancy relationships, the stress-strain behavior of sand under different stress levels is simulated. The coefficients $H_v + H_s$ preserve their roles like the base model (Pastor et al. 1990). That is, for dense sand, H_v and H_s start to reduce as shearing is initiated. H_v reaches zero when the critical state line is crossed (i.e., $H_v + H_s = 0$), and subsequently becomes negative. Immediately after the peak is reached, H_s reduces but H_v does not ($H_v + H_s < 0, H_L < 0$). H_s approaches zero at the critical state line upon further shearing.

The test results by Pradhan (1989) showed that the stress-dilatancy relationships under cyclic loading can also be expressed using an expression similar to Eq. (6)

$$d_g = (1 + \alpha)(M'_g - \eta) \quad (17)$$

$M'_g = M_g$ in loading but in unloading, it is expressed as

$$M'_g = \frac{6 \sin \phi_{cv}}{3 + \sin \phi_{cv} \sin 3\theta} \quad (18)$$

Upon unloading, the soil has been densified so that the plastic flow direction follows the following expression (similar to the original formulation):

$$\mathbf{n}_{gU} = \left(-abs \left(\frac{d_g}{\sqrt{1+d_g^2}}, \frac{1}{\sqrt{1+d_g^2}} \right) \right)^T \quad (19)$$

The pressure-dependent term and a term H_{den} are introduced into the unloading plastic modulus to consider densification and hardening behavior in the proposed model

$$H_u = H_{u0}(p'/p_a)^{0.5} \left(\frac{M_g}{\eta} \right)^{r_u} H_{den} \text{ for } \left| \frac{M_g}{\eta} \right| > 1$$

$$= H_{u0}(p'/p_a)^{0.5} H_{den} \text{ for } \left| \frac{M_g}{\eta} \right| \leq 1 \quad (20)$$

$$H_{den} = \exp(-r_d \varepsilon_{v0}^p) \quad (21)$$

where $r_u = \text{constant}$; and $\varepsilon_{v0}^p = \text{plastic volumetric strain at the instant of unloading or reloading, and it is either compressive or zero.}$

The reloading plastic modulus H_L is modified to account for the mean effective stress and past stress history

$$H_L = H_0(p'/p_a)^{0.5} H_f \{H_v + H_s\} H_{DM} H_{den} \quad (22)$$

where a stress memory factor H_{DM} is introduced to account for the history of past events. Three normalized deviatoric stress tensors are used to define H_{DM} : s_{ij}^u , s_{ij}^1 , and $s_{ij}^2 = \text{normalized deviatoric stress tensor at the last unloading, at the starting point of reloading, and at the second point of reloading, respectively}$

$$s_{ij}^u = e_{ij}^u / (p'_u M_{gu}) \quad (23)$$

$$s_{ij}^1 = e_{ij}^1 / (p'_1 M_{g1}) \quad (24)$$

$$s_{ij}^2 = e_{ij}^2 / (p'_2 M_{g2}) \quad (25)$$

where $e_{ij}^u = \text{deviatoric stress tensor at the last unloading; } p'_u = \text{corresponding mean effective stress; and } M_{gu} = M_g \text{ at that stress point. The superscripts and subscripts 1 and 2 state the quantities at the point of reloading and second point of reloading, respectively.}$

Two variables s_1 and s_2 are defined from above stress tensors leading to H_{DM}

$$s_1 = |s_{ij}^1 - s_{ij}^u| \quad (26)$$

$$s_2 = |s_{ij}^2 - s_{ij}^u|$$

$$H_{DM} = 1.0 \text{ when } s_1 > s_2$$

$$= \frac{1}{(1 + s_1)^r} \text{ when } s_1 \leq s_2 \quad (27)$$

where $r = \text{coefficient for the stress memory factor.}$

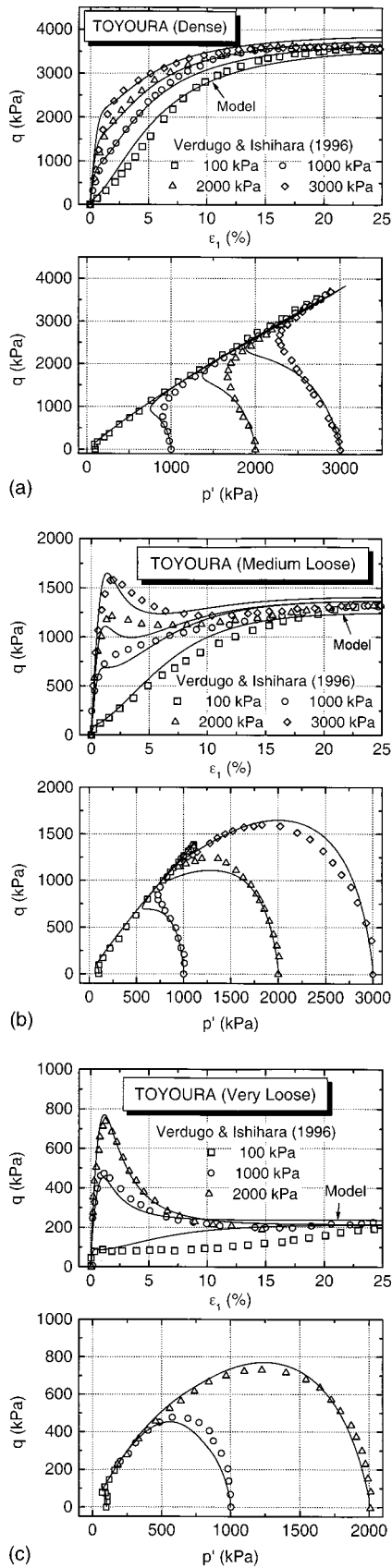


Fig. 3. Undrained triaxial compression tests on Toyoura sand: (a) dense, (b) loose, (c) very loose (experimental results after Verdugo and Ishihara 1996)

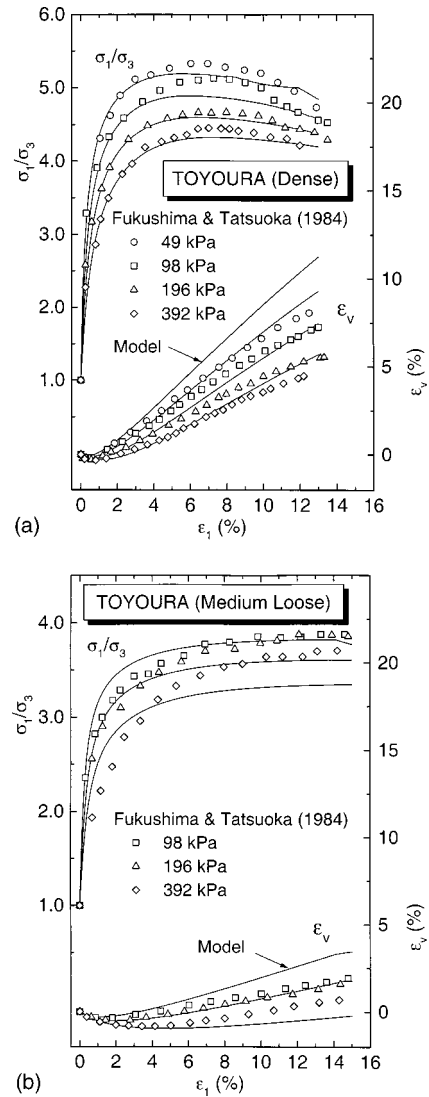


Fig. 4. Drained triaxial compression tests on Toyoura sand: (a) very dense, (b) medium loose (experimental results after Fukushima and Tatsuoka 1984)

Parameter Identification and Model Evaluation

A total of 15 parameters are needed to express proposed model considering cyclic loading. For the monotonic loading test, the total number is reduced to 11 (see Table 1). To identify the parameters, three drained or undrained triaxial tests having the same initial density are recommended. Two of the tests should be monotonic and having different initial confining pressures, and the other test should be conducted under cyclic loading. The difference in the confining pressure of the two monotonic tests should be large enough to cover the range of stress levels of interest. For advanced soil models that are different from simplistic models, which rely on a few conventional parameters, the calibration process becomes extremely important. A brief description of calibration procedure is given below.

The determination of G_0 , K_0 , ϕ_0 , $\Delta\phi$, and M_g is straightforward. G_0 is obtained from the stress-strain curve or from elastic wave propagation tests in the field or laboratory, such as the bender test. Triaxial tests with small strain measurement may also be used to quantify the elastic shear modulus. The empirical relationships similar to that of Hardin and Richard (1963) and Ishi-

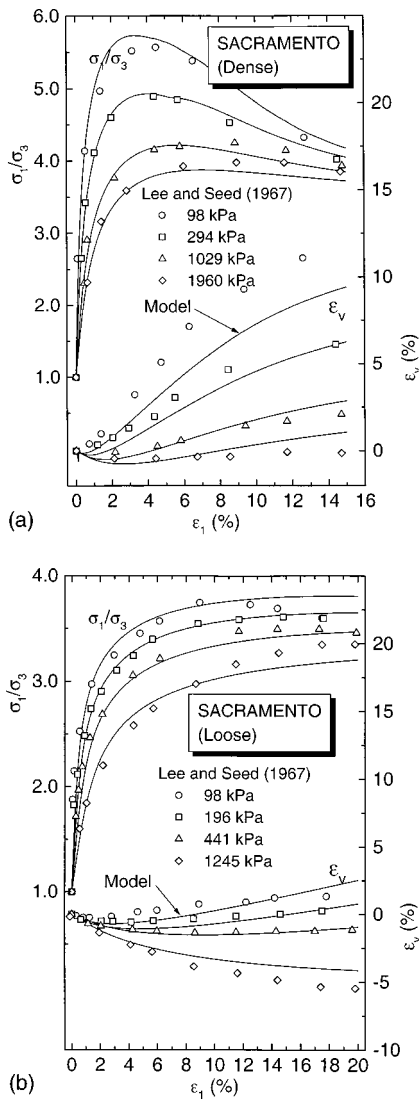


Fig. 5. Drained triaxial compression tests on Sacramento River sand: (a) dense, (b) loose (experimental results after Lee and Seed 1967)

hara (1996) may also be used to estimate the elastic modulus. K_0 can be obtained from isotropic compression test or by matching the initial slope of ϵ_1 or ϵ_v versus p' curve. The two elastic parameters, however, do not affect the response significantly. The terms ϕ_0 and $\Delta\phi$ can be obtained from Eq. (16) using the results of the two monotonic tests, which are conducted using different confining pressures (drained tests) or by fitting the stress–strain curves (undrained tests). M_g is equal to the stress ratio q/p' at the critical state of the monotonic triaxial tests.

M_f can be determined by fitting the results of the stress paths (q versus p') in undrained tests or ϵ_v versus ϵ_1 curve in the drained tests. The ratio M_f/M_g is larger for dense sand compared to loose sand. The term α is obtained from the slope of the stress ratio versus dilatancy curve. Its value is usually around 0.45; k_s is obtained from the two monotonic tests and the value is small for dense sand. H_0 is determined by fitting both the monotonic stress–strain curve and the ϵ_v versus ϵ_1 curve for drained tests or the $p'-q$ stress path for undrained tests. β_0 and β_{10} are determined by matching the stress–strain curves. An example of parametric study is given at the end of the paper.

There are four additional parameters for describing the cyclic behavior. H_{u0} is determined by fitting the results with the initial

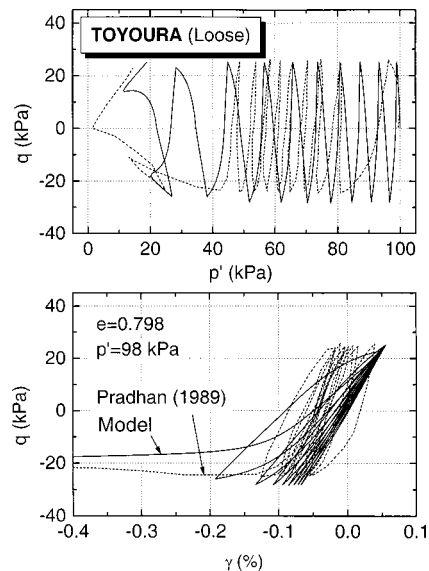


Fig. 6. Undrained cyclic loading test on loose Toyoura sand (experimental results after Pradhan 1989)

slope of the first unloading stress–strain curve; r_u is obtained by fitting the first unloading stress–strain curve; i is determined by matching the reloading curve in the cyclic test. For drained cyclic test, r_d is obtained by matching both the hysteretic loops in the stress–strain curve and $q - \epsilon_v$ curve. For undrained cyclic loading test, it can be determined by fitting the results with the stress path.

To assess the predictive capability of the proposed model, the simulation is compared with the published results of different kinds of sand under different initial densities: Toyoura sand (Fukushima and Tatsuoka 1984; Pradhan 1989; Verdugo and Ishihara 1996), Sacramento River sand (Lee and Seed 1967), Fontainebleau sand (Luong 1980), and Fuji River sand (Tatsuoka 1972). The densities of Toyoura sand used by these researchers were over a wide range of values, thus was conveniently called very dense ($e=0.67$), dense ($e=0.735$), medium loose ($e=0.831$), loose ($e=0.833$) and very loose ($e=0.907$). The parameters used for different types of tests are calibrated and summarized in Table 1. Note that several parameters were normalized by the atmospheric pressure to be dimensionless.

Monotonic Loading, Undrained Conditions

The undrained triaxial tests of Toyoura sand (Verdugo and Ishihara 1996) at three different relative densities were simulated and compared in Figs. 3(a–c): dense ($e=0.735, D_r=63.7\%$); loose ($e=0.833, D_r=37.9\%$); very loose ($e=0.907, D_r=18.5\%$). The confining pressure varied from 100 to 3,000 kPa. The deviatoric stress–strain relationships and stress paths are compared. The difference in response between the loose and dense states, i.e., from contractive to dilative behavior, was well described over this wide range of confining pressures. Note the slight deviation of excess pore pressure around the phase transformation line in the simulation of the dense and medium loose Toyoura sand that resulted in lower mean effective stress compared to the experimental results. The deviation, which is larger for higher confining pressure, was due to the assumption that the angles of phase transformation and critical state are the same. Also, as indicated by Lade and Yamamoto (1996), critical states are difficult to achieve as the confining pressure increases due to particle crushing.

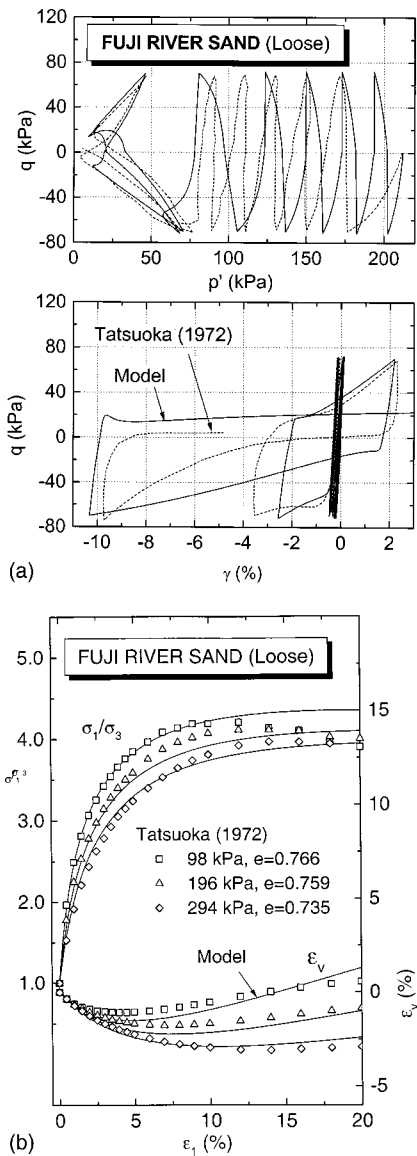


Fig. 7. Loose Fuji River sand: (a) undrained cyclic triaxial test, (b) drained monotonic triaxial test (experimental results after Tatsuoka 1972)

Monotonic Loading, Drained Conditions

Figs. 4(a and b) show the comparison of the model simulation with the drained triaxial tests for Toyoura sand (Fukushima and Tatsuoka 1984) at the dense ($e=0.67, D_r=82.5\%$) and medium loose ($e=0.831, D_r=39.2\%$) states, respectively. The confining pressures varied from 50 to 390 kPa for the dense state and 98–390 kPa for the medium loose state. Note that the simulation of medium loose Toyoura sand was based on the calibration of the undrained tests at the loose state of Verdugo and Ishihara (1996), which were of larger pressure levels. The comparisons for Sacramento River sand (Lee and Seed 1967) at the dense ($e=0.61, D_r=100\%$) and loose ($e=0.87, D_r=38\%$) states are presented in Figs. 5(a and b), respectively. The confining pressures were in the range of 98 to 1,960 kPa for the dense state and to 1,250 kPa for the loose state. The simulations are presented for both stress ratio and volumetric strain versus axial strain relationships under different stress levels. From the stress–strain relationships and the dilatancy curves, the proposed model showed the

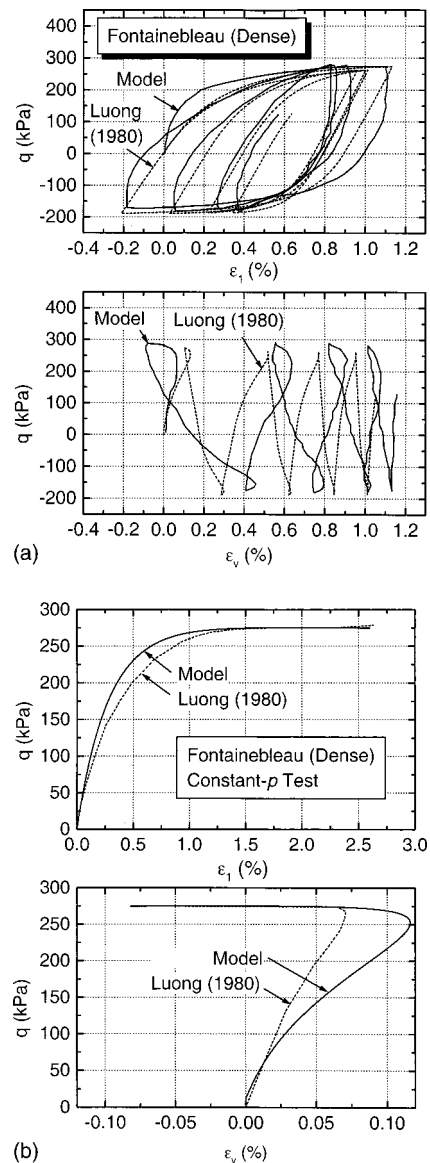


Fig. 8. Dense Fontainebleau sand, (a) Drained cyclic loading test, (b) constant- p' test (experimental results after Luong 1980)

contractive behavior of sand with an increase in the confining pressure. The model was also able to reproduce the dilative behavior at low confining pressure and the saturation of dilation as the confining pressure became large. The agreement between the simulations and test results for the two types of sand under different densities was very good.

Cyclic Loading, Undrained Conditions

The capability of the proposed model in simulating liquefaction and cyclic mobility of Toyoura sand (Pradhan 1989) and Fuji River sand (Tatsuoka 1972) are shown in Figs. 6 and 7, respectively. Toyoura sand was prepared at a loose state with $e=0.798, p'=98$ kPa and a constant stress amplitude of $q=\pm 25$ kPa. The void ratio of loose Fuji sand was $e=0.737$. The drained monotonic triaxial tests having an average void ratio $e=0.753$ were used to calibrate the basic 11 parameters [Fig. 7(b)]. Note that the parameters from the loose state of Verdugo and Ishihara (1996) were used to predict the behavior of loose Toyoura sand. Despite the complex behavior under undrained cyclic

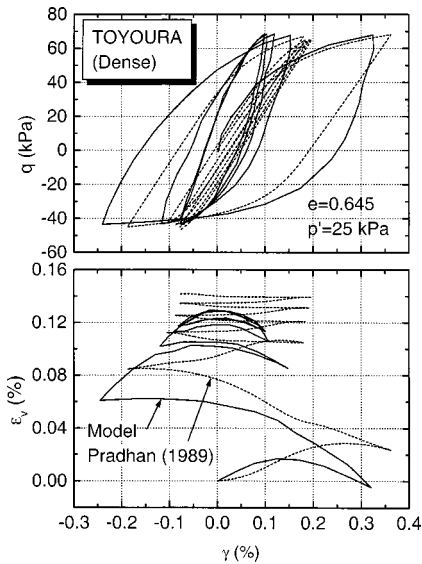


Fig. 9. Drained cyclic loading test on very dense Toyoura sand (experimental results after Pradhan 1989)

loading and slight difference between the densities of monotonic and cyclic tests, the model was able to simulate reasonably well the experimental results when compared to other models reported in the literature.

Cyclic Loading, Drained Conditions

A comparison is made for investigating the predictive capability of the model in simulating densification and hardening behavior of sand under cyclic loading. The model was used to simulate the behavior of a constant- p' triaxial test ($p' = 200$ kPa) of dense Fontainebleau sand ($e = 0.633, Dr = 65\%$) as reported by Luong (1980). The results obtained from a conventional triaxial test of very dense Toyoura sand ($e = 0.645, p' = 25$ kPa, with q/p' varying between 1.4 and -0.87 ; Pradhan 1989), were also compared. The monotonic drained triaxial test was used to calibrate the first 11 parameters for Fontainebleau sand [Fig. 8(b)], whereas that of Toyoura sand were based on Fukushima and Tatsuoka (1984). Figs. 8(a) and 9 show the comparison of simulated and experimental results for cyclic test of Fontainebleau and Toyoura sands, respectively. The model was able to simulate the cyclic hardening behavior of the sands reasonably well.

Sensitivity of Parameters

A series of parametric studies was conducted on Toyoura sand (very dense, $e = 0.67, p' = 98$ kPa, to investigate the effects of input parameters on the response. Since the effect of elastic moduli numbers G_0 and K_0 is not significant in static and cyclic loadings, only the effects of nine other monotonic related parameters are compiled and shown in Fig. 10. The response was plotted for the standard values of Table 1 (highlighted in dark) and two other values, one higher and the other lower than standard value) for each parameter. It can be seen that with the range of selected values, some parameters affect the strength (such as $\phi_0, \alpha, \beta_{10}, H_0, M_f$), whereas other parameters affect dilation (such as $\alpha, \beta_{10}, M_f, M_g$), shape of the curve before and after the peak strength, etc. Fig. 10 facilitates selection of parameters by varying the value in getting the desired response during calibration of

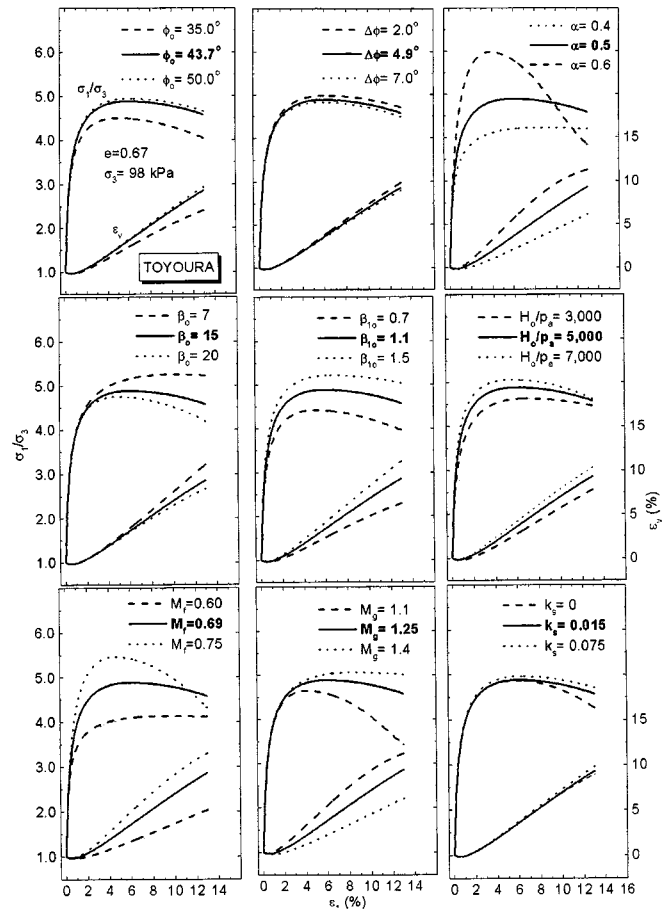


Fig. 10. Parametric studies on very dense Toyoura sand—drained triaxial test

other types of soil. However, the results of parametric studies here are limited to one confining stress and density of soil.

Summary and Conclusions

The generalized plasticity model for soil has been modified to consider pressure-level dependency. The capability of simulation was verified with the test results obtained from undrained and drained monotonic loading tests under different initial densities. The densification behavior under repeated loading has also been incorporated into the model and verified with the drained cyclic loading tests. The result of comparison was satisfactory, especially considering the case of Toyoura sand where the same set of parameters was used to predict the results of drained, undrained, and cyclic loading tests as reported by different researchers.

The model has to be calibrated with sand having an initial density of interest. Other effects, such as anisotropy and overconsolidation, are not considered. Comparison of the results having stress paths other than triaxial should also be conducted. The possibility of using a state parameter to unify the behavior of sand under different initial densities should be attempted. Further work has been conducted to implement the model for the analysis of well-controlled model tests (Ling et al. 2003).

Acknowledgments

The study was based upon work supported by the National Science Foundation Career Award under Grant No. CMS-0092739

with Dr. Clifford J. Astill as the Program Director. The soil model is developed for simulating the response of reinforced soil structures under earthquake loading. The reviewers have made several very useful comments leading to the improvement of the final manuscript. Professor Tatsuoka kindly provided his own thesis as well as a copy of Pradhan's thesis with the experimental works conducted at the Institute of Industrial science, University of Tokyo.

Notation

The following symbols are used in this paper:

- D_r = relative density;
 D^e, D^{ep} = elastic stiffness tensor, elastoplastic stiffness tensor;
 d_f, d_g = parameter related to loading direction vector, dilatancy;
 $d\varepsilon, d\varepsilon^e, d\varepsilon^p$ = incremental strain tensor, elastic strain increment, plastic strain increment;
 $d\varepsilon_s^p, d\varepsilon_v^p$ = incremental plastic deviatoric and volumetric strains;
 $d\sigma$ = incremental stress tensor;
 e = initial void ratio;
 $e_{ij}^1, e_{ij}^2, e_{ij}^u$ = deviatoric stress tensor at starting point of reloading, second point of reloading, at the last reloading;
 G_o, M_{gu} = elastic shear modulus, shear modulus number;
 H_{den} = densification coefficient in unloading plastic modulus;
 H_{DM} = stress memory factor in reloading modulus;
 H_f, H_v, H_s = plastic coefficients;
 H_0 = plastic modulus number;
 $H_{L/U}, H_L, H_U$ = loading or unloading, loading/reloading, unloading plastic modulus;
 H_{u0} = unloading plastic modulus number;
 K_{max}, K_0 = bulk modulus, bulk modulus number;
 k_s = parameter related to plastic coefficient H_s ;
 M_f = nonassociated flow parameter slope of failure line in p' - q plane;
 M_g, M'_g, M_{gu} = slope of critical state line in p' - q plane, M_g for cyclic loading, M_g at the stress point of last unloading;
 \mathbf{n} = loading direction vector;
 $\mathbf{n}_{gL/U}, \mathbf{n}_{gL}, \mathbf{n}_{gU}$ = flow direction vector under loading or unloading, loading, unloading;
 p', p'_u = mean effective stress, mean effective stress at last unloading;
 p_a = atmospheric pressure;
 q = deviatoric stress;
 r = coefficient related to H_{DM} ;
 r_d, r_u = parameter and exponent related to H_{den} and H_u ;
 s_1, s_2 = normalized deviatoric stress;
 $s_{ij}^1, s_{ij}^2, s_{ij}^u$ = normalized deviatoric stress tensor at starting point of reloading, second point of reloading, at the last unloading;
 α = parameter related to soil dilatancy;
 $\beta_0, \beta_1, \beta_{10}$ = parameters related to plastic coefficient H_s ;
 $\varepsilon_1, \varepsilon_3$ = major and minor principal strains;

- $\varepsilon_v, \varepsilon_v^p$ = volumetric strain, plastic volumetric strain at the instant of unloading or reloading;
 η, η_f = stress ratio q/p' , stress ratio parameter;
 η_p, η_{p0} = peak value of stress ratio, peak value of stress ratio at reference stress;
 θ = Lode's angle;
 σ_1, σ_3 = major and minor principal stresses;
 ξ = accumulative plastic deviatoric strain;
 ϕ_{cv}, ϕ_p = angle of internal friction at critical state, at peak; and
 $\phi_0, \Delta\phi$ = peak value of angle of internal friction at atmospheric pressure, change of angle with 10-fold increase in pressure.

References

- Bahda, F., Pastor, M., and Saitta, A. (1997). "A double hardening model based on generalized plasticity and state parameters for cyclic loading of sands." *Numerical models in Geomechanics*, Pietruszczak and Pande, eds., Balkema, Rotterdam, The Netherlands, 33–38.
- Banks, D. C., and MacIver, B. N. (1969). "Variation in angle of internal friction with confining pressure." *Rep. to U.S. Army Engineer Nuclear Cratering Group*.
- Bardet, J. P. (1986). "Bounding surface plasticity model for sands." *J. Eng. Mech.*, 112(11), 1198–1217.
- Been, K., and Jefferies, M. G. (1985). "A state parameter for sands." *Geotechnique*, 35(2), 99–112.
- Bolton, M. D. (1986). "The strength and dilatancy of sands." *Geotechnique*, 36(1), 65–78.
- Bouckovalas, G., Marr, W. A., and Christian, J. T. (1986). "Analyzing permanent drift due to cyclic loads." *J. Geotech. Eng.*, 112(6), 579–593.
- Boyce, H. R. (1980). "A nonlinear model for the elastic behavior of granular materials under repeated loading." *Proc., Int. Symp. on Soils under Cyclic and Transient Loading*, Swansea, U.K., 285–294.
- Crouch, R. S., Wolf, J. P., and Dafalias, Y. F. (1994). "Unified critical-state bounding-surface plasticity model for soil." *J. Eng. Mech.*, 120(11), 2251–2270.
- Crouch, R. S., and Wolf, J. P. (1994). "Unified 3D critical state bounding-surface plasticity model for soils incorporating continuous plastic loading under cyclic paths. Part I: Constitutive relations." *Int. J. Numer. Analyt. Meth. Geomech.*, 18, 735–758.
- Cuellar, V., Bazant, Z. P., Krizek, R. J., and Silver, M. L. (1977). "Densification and hysteresis of sand under cyclic shear." *J. Geotech. Eng. Div., Am. Soc. Civ. Eng.*, 103(5), 399–416.
- Dafalias, Y. F. (1986). "Bounding surface plasticity, I: Mathematical foundation and hypoplasticity." *J. Eng. Mech.*, 112(9), 966–987.
- Dobry, R., and Petrakis, E. (1990). "Micromechanics model to predict sand densification by cyclic straining." *J. Eng. Mech.*, 116(2), 288–308.
- Duncan, J. M., Byrne, P., Wong, K. S., and Mabry, P. (1980). "Strength, stress-strain and bulk modulus parameters for finite element analyses of stresses and movements in soil masses." *Geotechnical Engineering Research Rep. No. UCB/GT/80-01*, Dept. of Civil Engineering, Univ. of California, Berkeley.
- Fukushima, S., and Tatsuoka, F. (1984). "Strength and deformation characteristics of saturated sand at extremely low pressures." *Soils Found.*, 24(4), 30–48.
- Hardin, B. O., and Richart, F. E. (1963). "Elastic wave velocity in granular soils." *J. Soil Mech. Found. Div., Am. Soc. Civ. Eng.*, 89(1), 33–65.
- Houlsby, G. T. (1985). "The use of a variable shear modulus in elastic-plastic models for clays." *Comput. Geotech.*, 1, 3–13.
- Hueckel, T., Tutumluer, E., and Pellegrini, R. (1992). "A note on nonlinear elasticity of isotropic overconsolidated clays." *Int. J. Numer. Analyt. Meth. Geomech.*, 16, 603–618.
- Ibsen, L. B. (1999). "The mechanism controlling static liquefaction and cyclic strength of sand." *Physics and mechanics of soil liquefaction*,

- P. V. Lade, and J. A. Yamamuro, eds., Balkema, Rotterdam, The Netherlands, 29–39.
- Ishihara, K. (1996). *Soil behavior in earthquake engineering*, Oxford.
- Jefferies, M. G. (1993). “Nor-Sand: A simple critical state model for sand.” *Geotechnique*, 43(1), 91–103.
- Lade, P. V., and Kim, M. K. (1988). “Single hardening constitutive model for frictional materials. II yield criterion and plastic work contours.” *Comput. Geotech.*, 6(1), 13–30.
- Lade, P. V., and Yamamuro, J. A. (1996). “Undrained sand behavior in axisymmetric tests at high pressures.” *J. Geotech. Eng.*, 122(2), 120–129.
- Lee, K. L., and Seed, H. B. (1967). “Drained strength characteristics of sands.” *J. Soil Mech. Found. Div., Am. Soc. Civ. Eng.*, 93(6), 117–141.
- Li, X. S., Dafalias, Y. F., and Wang, Z. L. (1999). “State-dependent dilatancy in critical-state constitutive modelling of sand.” *Can. Geotech. J.*, 36(4), 599–611.
- Luong, M. P. (1980). “Stress-strain aspects of cohesionless soils under cyclic and transient loading.” *Proc., Int. Symp. Soils under Cyclic and Transient Loading*, Swansea, UK, 315–324.
- Maeda, K., and Miura, K. (1999). “Confining stress dependency of mechanical properties of sands.” *Soils Found.*, 39(1), 53–67.
- Manzari, M. T., and Dafalias, Y. F. (1997). “A critical state two-surface plasticity model for sands.” *Geotechnique*, 47(2), 255–272.
- Miura, N., Murata, H., and Yasufuku, N. (1984). “Stress-strain characteristics of sand in a particle-crushing region.” *Soils Found.*, 24(1), 77–89.
- Mroz, Z., and Zienkiewicz, O. C. (1984). “Uniform formulation of constitutive equations for clay and sand.” *Mechanics of engineering materials*, C. S. Desai and R. H. Gallagher, eds., Wiley, New York, 415–450.
- Nova, R., and Wood, D. M. (1979). “A constitutive model for sand in triaxial compression.” *Int. J. Numer. Analyt. Meth. Geomech.*, 3, 255–278.
- Pastor, M., Zienkiewicz, O. C., and Leung, K. H. (1985). “Simple model for transient soil loading in earthquake analysis. II: Non-associative models for sands.” *Int. J. Numer. Analyt. Meth. Geomech.*, 9(5), 477–498.
- Pastor, M., and Zienkiewicz, O. C. (1986). “A generalized plasticity, hierarchical model for sand under monotonic and cyclic loading.” *Numerical methods in geomechanics*, G. N. Pande, and van W. F. Impe, eds., Jackson, London, 131–150.
- Pastor, M., Zienkiewicz, O. C., and Chan, A. H. C. (1990). “Generalized plasticity and the modeling of soil behavior.” *Int. J. Numer. Analyt. Meth. Geomech.*, 14(3), 151–190.
- Pastor, M., Zienkiewicz, O. C., Xu, G. D., and Pinaire, J. (1993). “Modeling of sand behavior: Cyclic loading, anisotropy and localization.” *Modern approaches to plasticity*, D. Kolymbas, ed., Elsevier, New York, 469–492.
- Pestana, J. M., and Whittle, A. J. (1999). “Formulation of a unified constitutive model for clays and sands.” *Int. J. Numer. Analyt. Meth. Geomech.*, 23, 1215–1243.
- Ponce, V. M., and Bell, J. M. (1971). “Shear strength of sand at extremely low pressures.” *J. Soil Mech. Found. Div., Am. Soc. Civ. Eng.*, 97(4), 625–638.
- Pradhan, T. B. S. (1989). “The behavior of sand subjected to monotonic and cyclic loadings.” PhD thesis, Kyoto Univ., Japan.
- Prevost, J. H. (1978). “Plasticity theory for soil stress-strain behavior.” *J. Eng. Mech.*, 104(5), 1177–1194.
- Rowe, P. W. (1962). “The stress-dilatancy relation for static equilibrium of an assembly of particles in contact.” *Proc. R. Soc. London, Ser. A*, 269, 500–527.
- Sassa, S., and Sekiguchi, H. (2001). “Analysis of waved-induced liquefaction of sand beds.” *Geotechnique*, 51(2), 115–126.
- Silver, M. L., and Seed, H. B. (1971). “Deformation characteristics of sands under cyclic loading.” *J. Soil Mech. Found. Div., Am. Soc. Civ. Eng.*, 97(8), 1081–1098.
- Tatsuoka, F. (1972). “A fundamental study of the behavior of sand by triaxial testing.” PhD thesis, Univ. of Tokyo, Tokyo.
- Tatsuoka, F., Sakamoto, M., Kawamura, T., and Fukushima, S. (1986). “Strength and deformation characteristics of sand in plane strain compression at extremely low pressures.” *Soils Found.*, 26(1), 65–84.
- Tatsuoka, F., Siddiquee, M. S. A., Park, C. S., Sakamoto, M., and Abe, F. (1993). “Modelling stress-strain relations of sand.” *Soils Found.*, 33(2), 60–81.
- Verdugo, R., and Ishihara, K. (1996). “The steady state of sandy soils.” *Soils Found.*, 36(2), 81–91.
- Vermeer, P. A. (1978). “A double hardening model for sand.” *Geotechnique*, 44, 413–433.
- Vesic, A. S., and Clough, G. B. (1968). “Behavior of granular materials under high stresses.” *J. Soil Mech. Found. Div., Am. Soc. Civ. Eng.*, 94(3), 661–668.
- Wan, R. G., and Guo, P. J. (1998). “A simple constitutive model for granular soils: Modified stress-dilatancy approach.” *Comput. Geotech.*, 22(2), 109–133.
- Wang, Z.-L., Dafalias, Y. F., and Shen, C.-K. (1990). “Bounding surface hypoplasticity model for sand.” *J. Eng. Mech.*, 116(5), 983–1001.
- Yamamuro, J. A., and Lade, P. V. (1996). “Drained sand behavior in axisymmetric tests at high pressures.” *J. Geotech. Eng.*, 122(2), 109–119.
- Zienkiewicz, O. C., Leung, K. H., and Pastor, M. (1985). “Simple model for transient soil loading in earthquake analysis. I: Basic model and its application.” *Int. J. Numer. Analyt. Meth. Geomech.*, 9(5), 453–476.
- Zienkiewicz, O. C., and Mroz, Z. (1984). “Generalized plasticity formulation and applications to geomechanics.” *Mechanics of engineering materials*, C. S. Desai, and R. H. Gallagher, eds., Wiley, New York, 655–679.
- Zytynski, M., Randolph, M. F., Nova, R., and Wroth, C. P. (1978). “On modeling the unloading-reloading behavior of soils.” *Int. J. Numer. Analyt. Meth. Geomech.*, 2, 87–94.